Edinburgh Research Explorer

Aromatic reactivity revealed: beyond resonance theory and frontier orbitals

OPEN ACCESS

Aromatic Reactivity Revealed: Beyond Resonance Theory and Frontier Orbitals**‡

James J. Brown, and Scott L. Cockroft*

EaStCHEM, School of Chemistry, Joseph Black Building, University of Edinburgh, West Mains Road, Edinburgh, EH9 3JJ, UK.

[*]Corresponding author; e-mail: scott.cockroft@ed.ac.uk, tel: +44 (0)131 650 4758
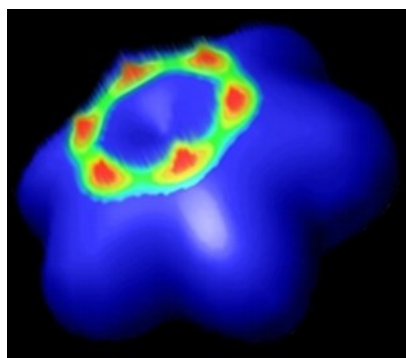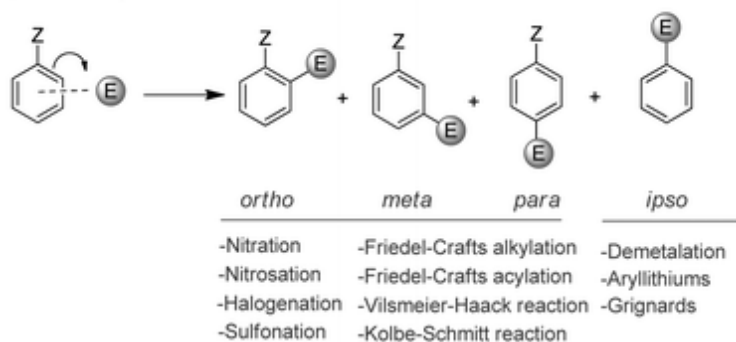
Graphical abstract:

Summary:
Ionisation energy surfaces consistently reveal the most reactive sites in aromatic molecules even where established reactivity models fail.
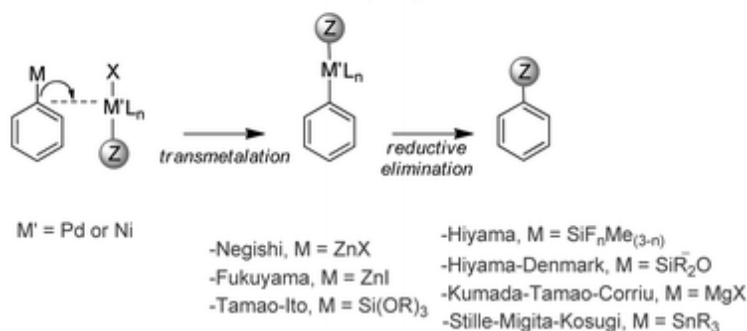
Abstract

The prediction of reactivity is one of the long-standing objectives of chemistry. We have extracted reactivity patterns observed in aromatic molecules spanning 150 years of synthetic developments and used the data to test the predictive capacity of popular reactivity models. This systematic analysis has exposed numerous regioselectivities that are not predicted by resonance theory, electrostatic potentials or frontier molecular orbital theory. In contrast, calculated local ionisation energy surfaces are shown to consistently reveal the most nucleophilic sites in aromatic molecules even where established reactivity models fail. Furthermore, these local ionisation energy minima are found to correlate with experimentally determined reactivity parameters. Since ionisation energy surfaces are simple to interpret and are provided as standard in popular computational chemistry software, the approach serves as a readily accessible tool for visualising the fundamental factors governing the reactivity of aromatic molecules.

a) **Electrophilic substitution**

ortho	meta	para	ipso
-Nitration	-Friedel-Crafts alkylation	-Demetalation	
-Nitrosation	-Friedel-Crafts acylation	-Aryllithiums	
-Halogenation	-Vilsmeier-Haack reaction	-Grignards	
-Sulfonation	-Kolbe-Schmitt reaction		

b) **Transmetalation in cross-coupling reactions**

M' = Pd or Ni

-Negishi, M = ZnX
-Fukuyama, M = ZnI
-Tamao-Ito, M = Si(OR)$_3$

-Hiyama, M = SiF$_n$Me$_{(3-n)}$
-Hiyama-Denmark, M = SiR$_2$O
-Kumada-Tamao-Corriu, M = MgX
-Stille-Migita-Kosugi, M = SnR$_3$

c) **Electrophilic addition**
(in reactive aromatics with double-bond character)

-Oxidation
-Oxymercuration
-Michael addition

-Hydrohalogenation
-Hydrogenation
-Dihalogenation
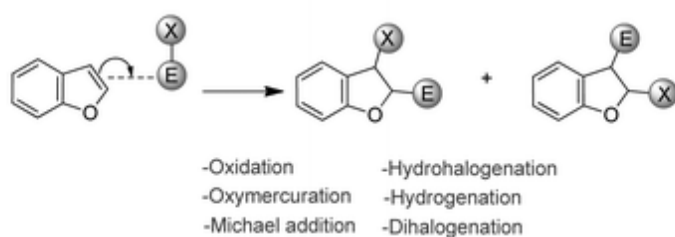
Introduction

The prediction of reactivity is one of the cornerstones of synthetic chemistry. The intrinsic link between theory and experiment is particularly well-illustrated by the chemistry of aromatic molecules, which has played a pivotal role in shaping foundational concepts such as valence bond theory,[1, 2] substituent effects,[3, 4] resonance theory,[5] and Frontier Molecular Orbital (FMO) theory.[6, 7] Indeed, the exploration of chemical diversity in pharmaceuticals, agrochemicals, and materials depends upon methods for predicting and directing the regiochemistry of aromatic functionalisation reactions (Fig. 1).[8-15]

← *Figure 1.* Routes of electrophilic attack in aromatic functionalisation reactions.

The chemistry of aromatic molecules is typified by the reactions of their π-systems with electrophiles (Figs. 1 and 2). Such reactions are often rationalised using empirical reactivity rules derived from resonance theory,[5] or calculated properties such as FMOs[6, 7] and electrostatic potentials.[16, 17-19] Here we show that none of these popular methods offer a comprehensive solution to the prediction of aromatic reactivity (Figs. 4, S3 and S15). Instead, our analysis of thousands of experimental observations of electrophilic substitution, addition and transmetalation reactions, has revealed average local ionisation energy (IE) surfaces as a more reliable, yet simple model for visualising the reactivity of aromatic molecules under kinetic control (Figs. 4-6, and S1-14). Furthermore, correlations with experimentally determined reactivity parameters show that the model can provide quantitative predictions of the relative nucleophilicities of aromatic molecules (Fig. 3).

Electrophilic aromatic substitution (EAS) reactions serve as classic but appropriate starting point for considering the reactivity of aromatic molecules (Fig. 1a). Most EAS reactions follow a simple kinetically controlled mechanism with a clearly defined initial rate-determining step (Fig. 2).[20] Thus, the kinetic reactivity of an aromatic molecule is governed by the energy difference between the ground-state reactants and the transition state (TS1) on forming the resonance-stabilised arenium intermediate. Modern computational methods can be used to predict the regiochemical outcome of EAS reactions by calculating the energy differences between the ground-state reactants and the transition state for each regiochemical reaction pathway.[21] However, widespread adoption of such methods may be hindered by the technical requirements and specialist training needed to perform these types of calculations. Indeed, effective application of theoretical methods in synthetic chemistry depends on striking the correct balance between the predictive capacity of the model and the ease with which it can be applied. As a result, chemical reactivity is still frequently rationalised using resonance theory and simple calculated properties such as electrostatic potentials[16, 17-19] and frontier molecular orbital-based methods.[6, 7, 22, 23] Here we use experimental literature data to examine the utility of these simple methods in understanding the reactivity of aromatic molecules.
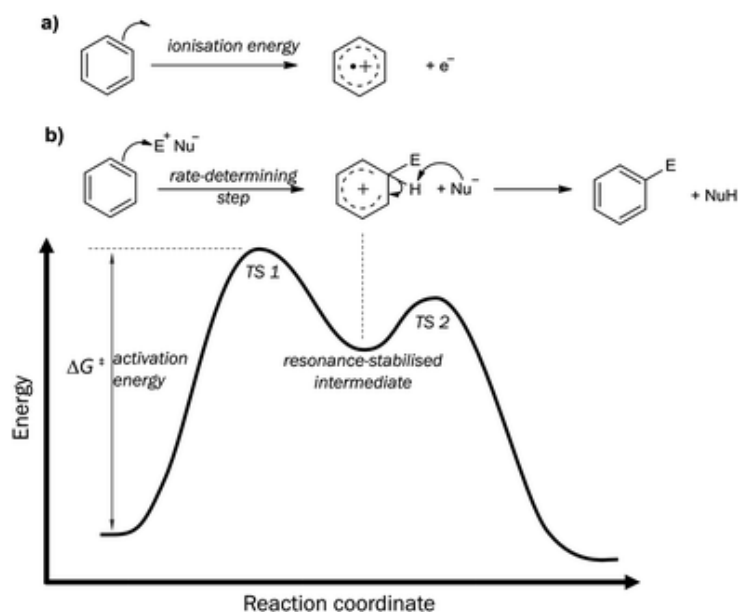
Figure 2. The mechanism of electrophilic aromatic substitution (EAS) and its relationship with ionisation energies. a) Scheme showing ionisation via the removal of a single electron. b) Scheme showing a typical reaction mechanism for EAS and the corresponding reaction energy profile.

Ionisation Energies as a Reactivity Descriptor

Although simple calculated properties such as HOMOs, LUMOs and electrostatic potentials are frequently encountered alongside discussions of reactivity, ionisation energy surfaces (which are one of the other standard molecular surfaces found in off-the-shelf computational software packages), are hardly ever seen. Thus, before examining the utility of often-used reactivity models it is worth considering whether ionisation energy surfaces might be of any use in understanding the reactivity of aromatic molecules.

The relationship between ionisation energies (IEs) and chemical reactivity has long been recognised with regards to the relative reactivities of the elements.[24] More recently, Politzer and co-workers developed a method of calculating so-called average local ionisation energies $\bar{I}(\mathbf{r})$;

$$\bar{I}(\mathbf{r}) = \frac{\sum_i \rho_i(\mathbf{r})|\epsilon_i|}{\rho(\mathbf{r})} \qquad \text{(Eqn 1)}$$

Where $\rho_i(\mathbf{r})$ is the electronic density of the orbital with energy ϵ_i at point $\mathbf{r}$, and $\rho(\mathbf{r})$ is the total electronic density.[25] When this property is plotted on a molecular surface it is denoted as $\bar{I}_S$, and it can be interpreted as the average energy needed to remove an electron from that position on the molecule. Thus, it has been proposed that the location of the IE minimum on this surface, $\bar{I}_{S,min}$ corresponds to the site most likely to react with an electrophile.[25]

Expanding upon this concept, Fig. 2 highlights the similarity of the ionisation process to the formation of the cationic arenium intermediate in the rate-determining step of an EAS reaction. Thus, to test whether the energy change in the rate-determining step of EAS reactions is approximated by calculated average local IEs, we correlated these calculated energies against quantitative experimental measures of the reactivity of aromatic molecules with electrophiles (Fig. 3). An excellent correlation was found between calculated local IEs taken over the *meta* and *para* positions of mono-substituted benzenes and Hammett substituent constants, which are established as one of the most successful empirical descriptors of reactivity in aromatic molecules (Fig. 3a, Table S1).[26]
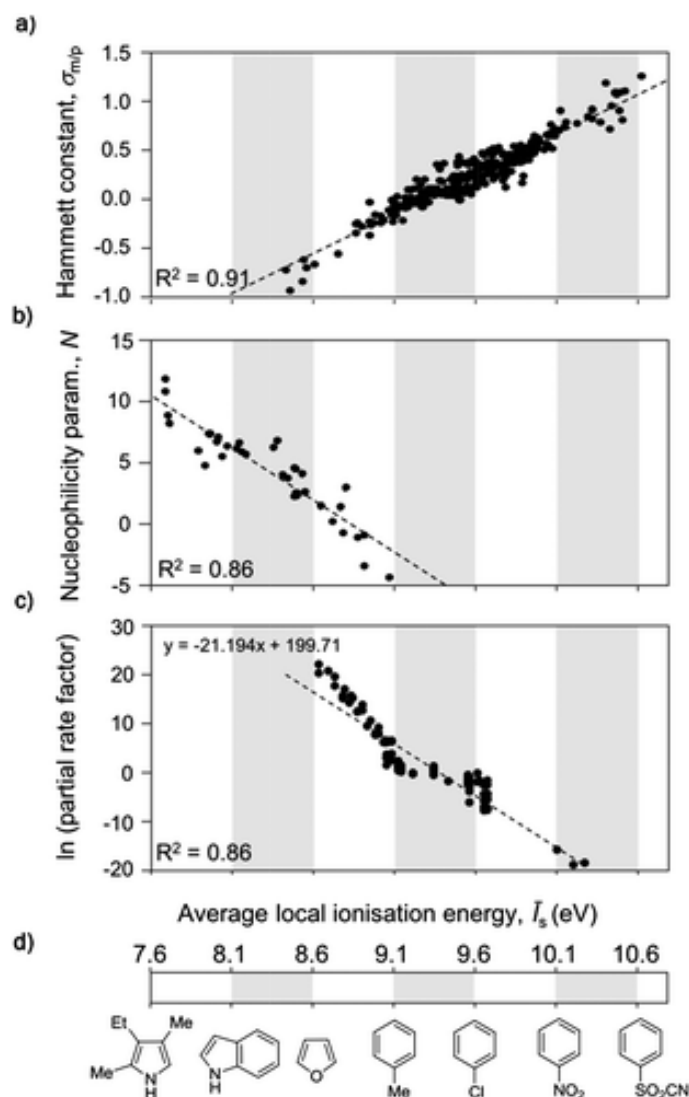
Figure 3. Correlations of average local ionisation energies calculated using B3LYP/6-311G* with experimental reactivity parameters. a) Hammett substituent constants. b) Mayr's Nucleophilicity parameters. c) Partial rate factors for electrophilic substitution reactions at different carbon positions in benzene derivatives. d) A scale of average local ionisation energies including representative examples. Numerical data and references are provided in Supporting Tables S1-S3.

High-quality kinetic data obtained under controlled conditions is required for further validation of local ionisation energies. Mayr and co-workers have made great progress towards the establishment of a standard scale of nucleophilicity.[27] Fig. 3b shows that local IE minima correlate with Mayr's nucleophilicity parameters for a range of multiply-substituted benzenes, indoles, thiophenes, furans, and pyrroles. The correlation is reasonable considering that these data were determined in one of two different solvents (dichloromethane or acetonitrile) and the effects of multiple reactive sites with different steric demands are not taken into account.

Local IEs plotted against experimentally determined partial rate factors for a range of electrophilic aromatic substitution reactions including nitration, bromination, chlorination, mercuration, ethylation and benzylation reactions are plotted in Fig. 3c. Overall a pleasing correlation is observed considering that the data were obtained from multiple sources and the range of reactions covered. Indeed, subsets of the data obtained in individual studies yield correlation coefficients $R^2 = 0.95$ - 0.99 (Fig. S18). Despite the simplicity of the IE model, these correlations compare well with plots of the same data against calculated 'Electrophile Affinities' (Table S2).[21] This supports the hypothesis that calculated average local IEs approximate the energy change in the rate-determining step for each regiochemical pathway (which is rigorously calculated in the Electrophile Affinity model).

Fig. 3c allows a quantitative relationship to be formed between calculated local IE values and experimental partial rate factors, which in turn can be used to calculate the expected % yields of different regioisomers as follows:

$$predicted \text{ \% yield at position } j = \frac{n_j \exp(m \, \bar{I}_{S,j})}{\sum_j n_j \exp(m \, \bar{I}_{S,j})} \times 100\% \qquad \text{(Eqn 2)}$$

where n_j is the number of equivalent aromatic positions j that are available for substitution, m is the gradient of the graph determined in Fig. 3c ($m = -21.194$), and $\bar{I}_{S,j}$ is the average local ionisation energy taken over each position j.

The accurate prediction of regioisomer ratios by this approach presents a number of potential challenges. Firstly, yields are often dependent on the nature of the electrophile and steric effects, which are not accounted for in the IE model. Secondly, since small changes in the IEs result in exponential changes in the relative rates of reaction at different sites, the prediction of regioisomer ratios may be associated with significant errors. Nonetheless, the assertion that Eqn 2 might be used for the semi-quantitative prediction of regioisomer yields is supported by Figure S19, which shows that yields can be predicted with an accuracy of ±25% for all but the most sterically hindered substrates.

Ionisation Energy Surfaces for Visualising Regioselectivity Patterns in Aromatic Molecules

Although regioisomer yields could be predicted using Eqn 2, experimental variations often limit the reproducibility of yields such that high-quality kinetic data are not obtained, or indeed required during routine chemical syntheses. Thus, perhaps more a more pragmatic, and easily accessible approach might take advantage of the ability to plot local IE energies on the surface of a molecule, in a similar fashion as electrostatic potentials.[25] Clearly, if average local IE energies correlate with the kinetics of electrophilic

substitution reactions in different positions of aromatic molecules (Figure 3), then the most reactive sites will be revealed when the property is plotted on a molecular surface, provided that an appropriate colour scale is selected. In this way, the IE model should provide a means of visualising the fundamental electronic factors governing the reactivity of aromatic substrates.

The IE surfaces presented in the current work are scaled such that minima are highlighted in red ($\bar{I}_{S,min}$), while at the opposite end of the scale, blue corresponds to sites where negligible experimental reactivity with electrophiles is seen ($\bar{I}_S > \bar{I}_{S,min}$ +0.4 eV) (Table 1, Figs. 4-6 and those in the SI). A step-by-step guide showing how these surfaces are generated is provided in the Supporting Information.

Average local IE at position j $\bar{I}_{S,j}$/eV	Colour of IE surface at position j	Approx. regioisomer yield
$\bar{I}_{S,min}$	red	>50%
$\bar{I}_{S,min}$ + 0.05 to +0.1	orange/yellow	<50%
$\bar{I}_{S,min}$ + 0.2	green	<25%
$\bar{I}_{S,min}$ + 0.4	blue	negligible

Table 1. Optimised colour scale for visualising ionisation energy surfaces and the associated approximate regioisomer yield predictions.

This optimised scale was selected based on the large-scale analysis of experimentally observed reactivity patterns presented in this work, and reveals secondary reactive sites in shades of orange/yellow (and occasionally green) alongside the most reactive sites, which are highlighted in red. This approach facilitates the prediction of approximate regioisomer distributions (that are consistent with Eqn 2) via rapid visual inspection of calculated IE surfaces (Table 1). One advantage of this approach over some other computational methods is that regiochemical preferences can be quickly assessed without the requiring separate calculations for each regiochemical reaction pathway.

Ionisation Energy Surfaces and Reactivity Patterns in Monosubstituted Benzenes

The effects of substituents on the regioselectivity of electrophilic aromatic substitution reactions in benzene derivatives serve as an excellent test-bed for examining the predictive utility of IE surfaces relative to other established methods. These reactivity patterns are often summarised as a set of empirical rules derived from

resonance theory, and state that substituents which withdraw electron density via resonance direct attack to the *meta*-positions, while substituents that donate electron density through resonance or hyperconjugation are *ortho*/*para*-directing.[8] Such rules work well in simple cases where reactivity is governed by resonance, but the generality of this approach is limited because inductive effects are not always negligible. For example, halogens are frequently classified as weakly deactivating (via the inductive effect), but *ortho*/*para*-directing (due to resonance). However, closer examination of the experimental data reveals that halogenobenzenes are significantly more likely to react with an electrophile in the *para*-position relative to the *ortho*-positions, despite there being two *ortho*-positions and only one *para* position (compound **1**, Fig. 4a).[28, 29, 36] Resonance theory is therefore unable to differentiate between the reactive behaviour of chlorobenzene, **1** which reacts with electrophiles mostly in the *para*-position and the phenoxide anion **2**, which reacts primarily in the *ortho* position (Fig. 4b).[29, 31, 32, 37] In contrast, the calculated average local ionisation energy (IE) surfaces of molecules **1-3** in Fig. 4 correspond well with the observed reactive behaviour. In halobenzenes, it can be hypothesised that both *ortho* and *para* positions are activated by resonant electron donation from the lone-pair electrons on the halogen substituent, but the competing inductive influence of the electronegative halogen reduces the nucleophilicity of the nearby *ortho* positions more than the *para* position. In the case of phenoxide **2** it can be proposed that similar resonant effects come into play, but the *ortho* positions are more inductively activated than the *para* position.
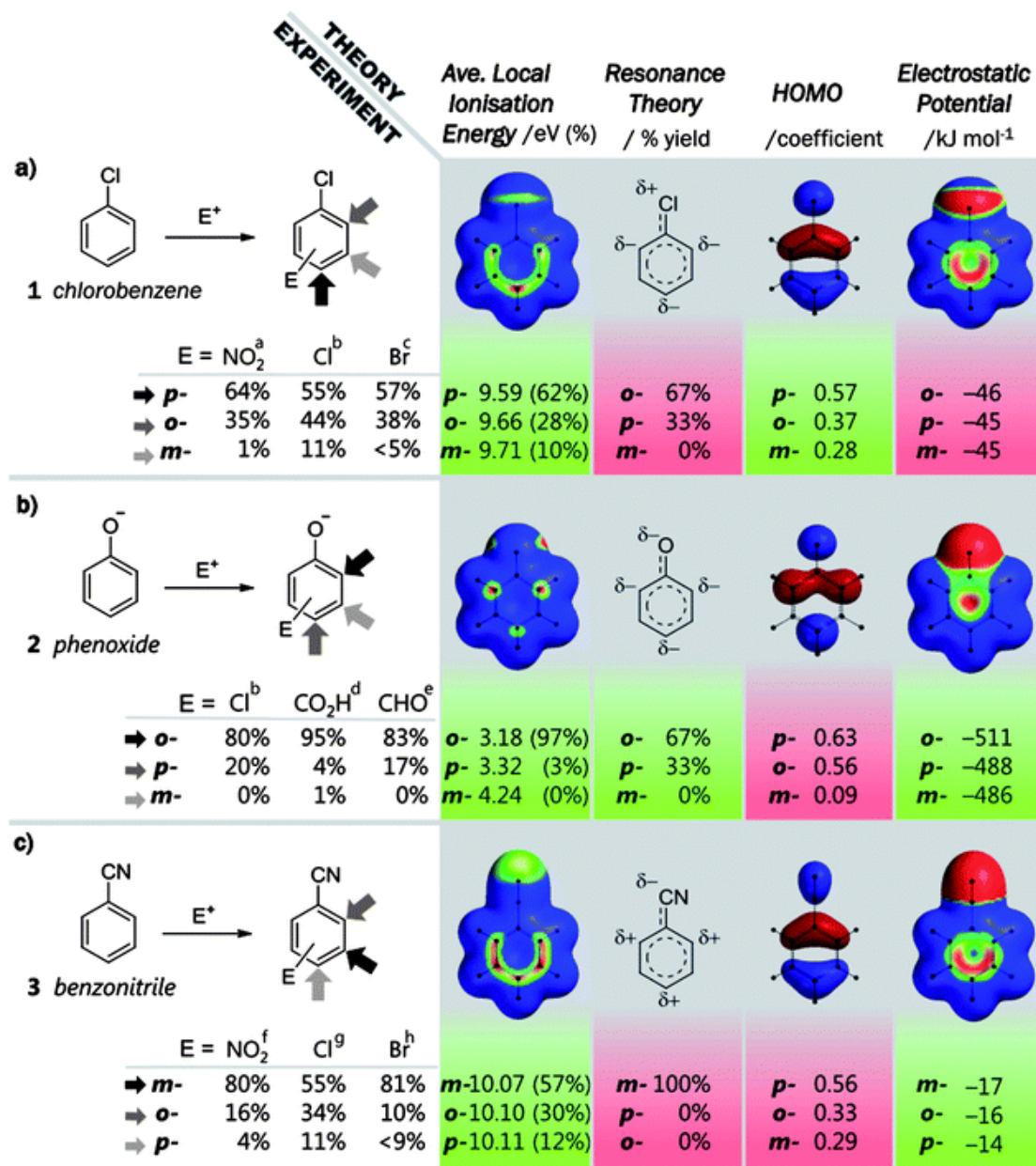
Figure 4. A comparison of regioselectivity in electrophilic aromatic substitution reactions vs. theoretical descriptors. The positions of the ionisation energy minima on the molecular surfaces ($\bar{I}_{S,min}$, red) correspond with the experimentally determined nucleophilic sites, even where predictions based on resonance theory, FMO theory (HOMOs) and electrostatic potentials fail (red background shading). Blue regions of the ionisation energy (IE) surfaces represent all regions where the local IE is $> \bar{I}_{S,min}$ +0.4 eV. The electrostatic potential surfaces are scaled from the lowest potential on each aromatic ring (red) to this value plus 15 kJ mol^{-1} (blue). Values shown underneath the theoretical structures correspond to the *ortho*, *meta* and *para* positions as indicated. Further comparisons are presented in the Supporting Information. All molecular surfaces were calculated using Spartan '08 with B3LYP/6-311G*. Percentage yields estimated from IE values were calculated using Equation 2 and are associated with an error of up to ±25% (Fig. S19). References for the reactions shown: a[28], b[29], c[30], d[31], e[32], f[33], g[34], h[35].

The propensity of the phenoxide anion **2** (Fig. 4b) to react with electrophiles in the *ortho* position is shared by the benzoate anion **4** (Fig. 5). This reactivity pattern was first reported in the 1930s,[38] but has seen renewed interest in recent synthetic methodologies.[15, 39] Such *ortho*-reactivity is often rationalised as arising through-coordination of the incoming electrophile via an oxygen atom.[29] However, the IE surfaces support the initial, but often-overlooked hypothesis presented in the original publication,[29] that the *ortho* positions in these molecules are intrinsically more nucleophilic as a result of inductive effects. Resonant donation of electron density into the *ortho* and *para* positions can occur in phenoxide, **3**, but no equivalent canonical forms can be drawn for the benzoate anion **4**. Accordingly, while the IE surface of the phenoxide anion **3** (Fig. 4b) shows a secondary reactive site over the *para* position, this is absent in the benzoate anion, **4** (Fig. 5a). Inductive effects are not apparent in the IE surface of anisole, **5** whose textbook, resonance-dominated reactivity is reflected in the similar IE energies seen over the *ortho* and *para* positions. These observations support the hypothesis that positions *ortho* to an anionic substituent are mostly activated via the inductive effect.
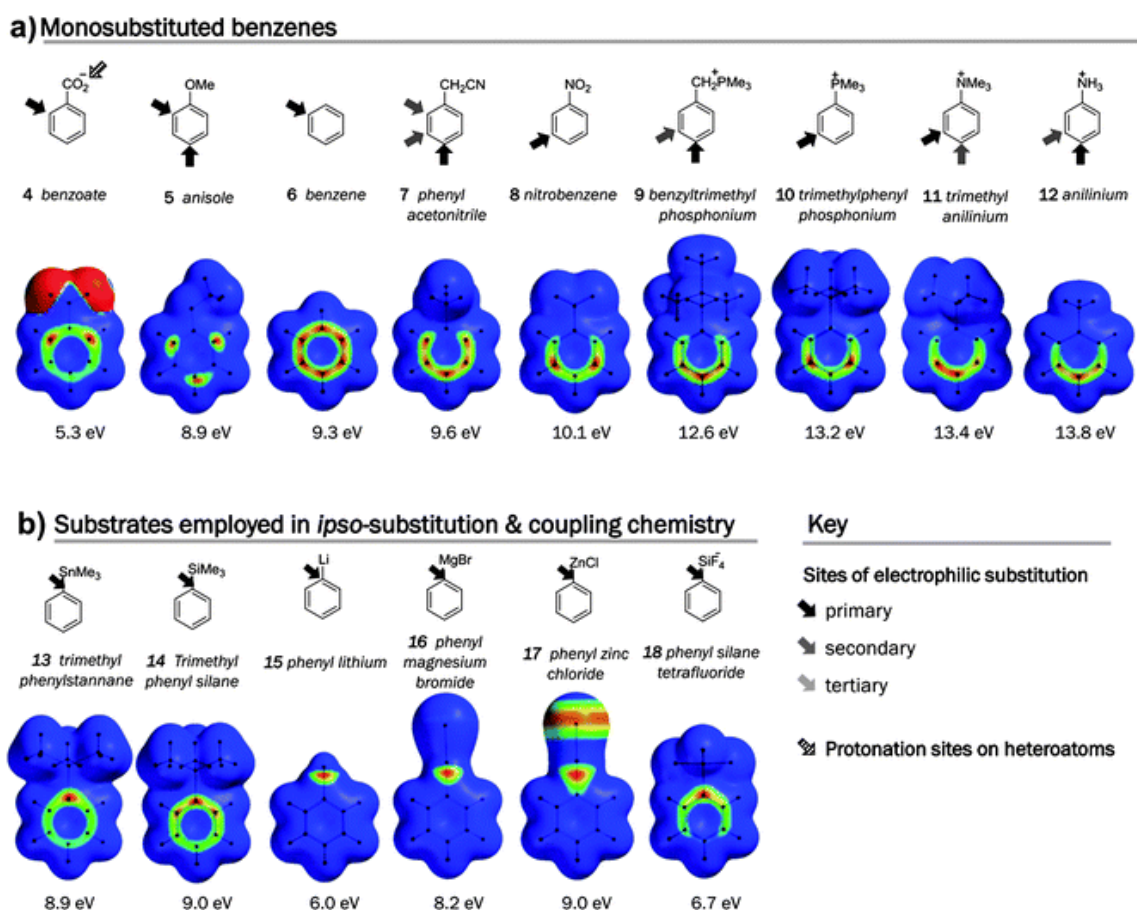

Figure 5. Experimental reactivity patterns and corresponding calculated average local ionisation energy surfaces and minimum values ($\bar{I}_{S,min}$) for a range of mono-substituted benzenes, other examples are shown in Fig. 4. References for all reactivity patterns and many other examples are presented in the Supporting Information.

While electrostatic potentials (ESPs) might be expected to take resonant and inductive effects into account, Fig. 4 shows that ESPs do not provide a useful indicator of reactivity since the electrostatic minima (red regions in Figs. 4 and S3) are often located over unreactive substituents. In addition, ESP values taken over the *ortho*, *meta* and *para* positions of chlorobenzene **1** do not vary in relation to their reactivities (Fig. 4a).

In accord with predictions derived from resonance theory, benzonitrile **3** reacts predominantly in the *meta* position (Fig. 4c). However resonance theory fails to provide an explanation for the significant *ortho*-reactivity observed in this molecule.[33, 34, 36] This reactivity pattern is difficult rationalise, yet the IE surfaces correspond with this observation and show significant streaking of lower IE energies from the *meta* positions across the *ortho* positions (but much less so across the *para* position). At this point it is worth mentioning that the largest HOMO lobe lies over the *para* position in benzonitrile **3**, (Fig. 4c). Thus, frontier molecular orbital (FMO) theory incorrectly predicts *para*-substitution in benzonitrile **3**, despite the method serving as a powerful tool for predicting the outcome of many organic reactions, and pericyclic reactions in particular.[40]

Based on classic reactivity rules, one might predict cationic substituents to be *meta*-directing due to their powerful electron-withdrawing properties. This holds true for benzene rings bearing PMe_3^+, $AsMe_3^+$, $SbMe_3^+$, SMe_2^+ SPh_2^+, and $SeMe_2^+$ substituents, but it has been shown that OPh_2^+, $CH_2PMe_3^+$ and NH_3^+ direct primarily to the *para* position and secondly to the *meta* position (compounds **9-12**, Figs. 5a and S4).[41] It is difficult to rationalise these differences using established reactivity models, but each of these reactivity patterns are correctly predicted by calculated IE surfaces, including the intermediate behaviour of NMe^{3+} which directs mostly to the *meta* position and partially to the *para* position (Figs. 5a and S4).

A more subtle but interesting example is provided by phenylacetonitrile **7**, which bears a weakly electron-withdrawing CH_2CN substituent,[26] that is predominantly *para*-directing, but also gives moderate yields of both *ortho*- and *meta*-products,[42] as is represented in the IE surface (Fig. 5a).

Moving to the opposite electronic extreme, some inductively electron-donating substituents undergo *ipso*-substitution in which the incoming electrophile replaces the directing group. Typical examples of molecules expressing such behaviour include trialkyl phenyl stannanes and silanes which have IE minima located over the *ipso* position (compounds **13-14** in Fig. 5b). Some of the most useful *ipso*-substitution reactions employ metals with low electronegativities, which increase the nucleophilicity of aromatic rings to such an extent that reactions with weak electrophiles become possible. Prominent examples include synthetic strategies that make use of lithiated species **15**,[9] and Grignard reagents **16**,[14] which accordingly have very low calculated average local ionisation energies (Figs. 5b and S5).

Many important synthetic transformations involve a catalytic cycle featuring a transmetalation step. Transmetalation is proposed as involving electrophilic attack of a catalytic metal at the α-carbon, *ipso* to the metalated position on the aromatic ring (Fig. 1b).[14] Substrates proposed as undergoing transmetalation in such a manner include the aforementioned magnesium halides in Kumada-Tamao-Corriu reactions (**16**), zinc

halides (**17**) in Negishi and Fukuyama couplings, stannanes in Stille-Migita-Kosugi reactions (**13**), and silanes in the Tamao-Ito and Hiyama couplings (**14** and **18**).[14] Ionisation energy surfaces of examples of these substrates are collated in Figs. 5b and S5 and in all cases the average local ionisation energy minima are located over the *ipso*-carbon. Such a prediction could not be derived from resonance theory, FMOs or ESPs (Fig. S3).

Large-scale Examination of Substrate Scope of Ionisation Energy Surfaces

Thus far we have only considered reactivity patterns in monosubstituted benzenes, but heteroatoms and multiple substituents might be expected to complicate the prediction of reactivity patterns. Encouraged by the correlations in Fig. 3 (which includes data for heteroaromatic and multiply-substituted compounds), and the ability of the IE method to account for both major and subtle reactivity patterns in monosubstituted benzenes as discussed above, we set about performing a systematic validation of average local ionisation energies against experimental reactivity data for a broader range of substrates.

Since experimental yields are usually only reported for the major isomers of a reaction, generalised reactivity patterns extracted from literature observations provide the most practical means of assessing the scope and utility of the IE approach across the broadest possible range of aromatic substrates. Fully referenced reactivity patterns are presented alongside calculated IE surfaces for over one hundred metalated, heterocyclic, polycyclic and multiply-substituted aromatics in Figs S1-S14. Fig. 6 highlights several particularly challenging examples where well-established reactivity models are known to fail. Despite their challenging nature, the IE surfaces agree with the observed reactive behaviour even where resonance theory, FMO theory, Brown's selectivity relationship, the Fukui function and electrostatic models fail.[17, 18]

1,2,4-trimethylbenzene **19** has been shown to violate Brown's empirical 'selectivity relationship', which uses Hammett substituent constants to make quantitative predictions of substitution patterns in multiply-substituted benzenes.[43] In this case, the selectivity relationship predicts the 5- and 6-positions to be equally reactive, but experimentally, electrophilic substitution is preferred in the 5-position, then the 3-position and finally the 6-position.[44] The IE surface shown in Fig. 6a provides a good account of these preferences even though steric differences between the 5- and 3- positions are clearly not taken into account on the IE surface. This suggests that the selectivity relationship fails due to fundamental electronic factors rather than as a result of the previously proposed atypical reaction mechanism.[45]

Nitration of 1-nitronaphthalene **20** is favoured in the 8-position over the less sterically hindered 5-position, but resonance theory and FMO theory predict equal electronic reactivity in the 5- and

8-positions (Fig. S15). Consistent with the experimental result, the calculated IE surfaces clearly indicate the 8-position to be the more nucleophilic site (Fig. 6a).[46]   The dihydro-1,4-diazepinium cation **21** has been

described as quasi-aromatic due to its propensity to undergo electrophilic substitution reactions similar to those of true aromatic substrates. These unusual substitution reactions are highly-selective for the 6-position and accordingly the calculation ionisation energy minimum is neatly localised over this position (Fig. S13).[47]
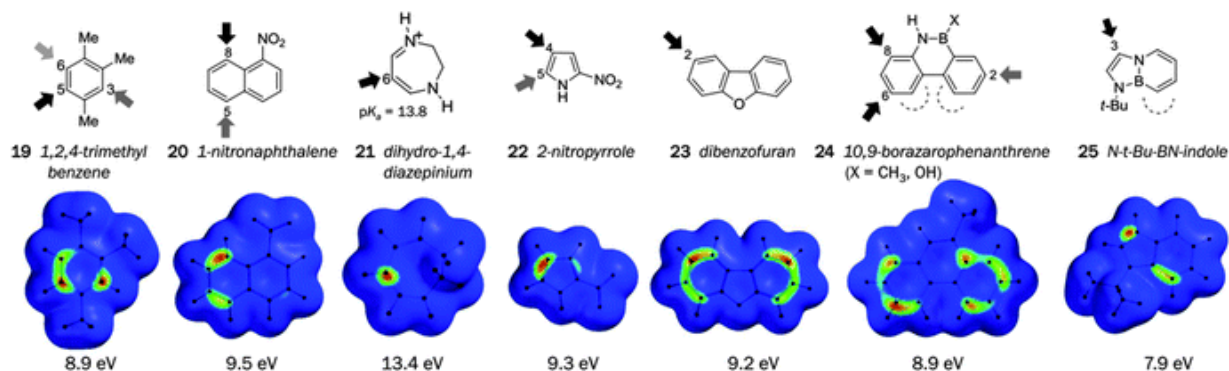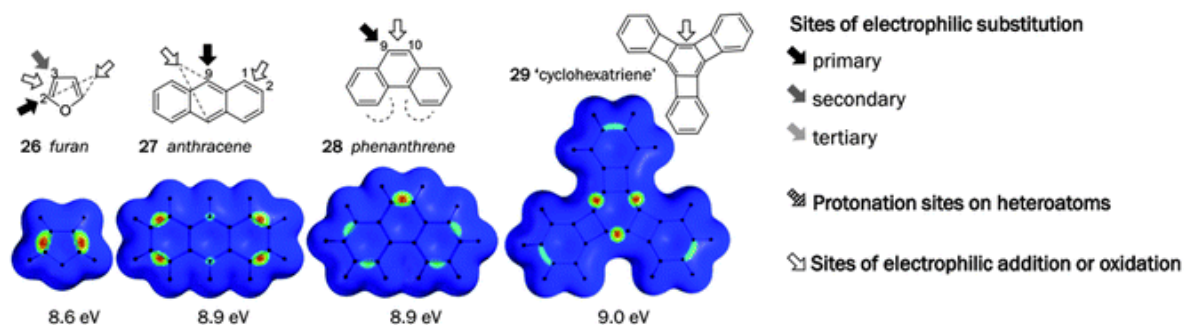

Figure 6. Experimental reactivity patterns and corresponding calculated average local ionisation energy surfaces and minimum values ($\bar{I}_{S,min}$) for a range of aromatic molecules. References for all reactivity patterns and many other examples are presented in the Supporting Information.

2-Substituted thiophenes and furans react predominantly in the 5- position whether the substituent is electron donating or withdrawing (see the many references in Fig. S8). In contrast, pyrrole rings bearing electron-withdrawing substituents in the 2-position react in the 4-position (e.g. compound **22** in Fig. 6a).[48-51] Ionisation energy surfaces correctly predict this exceptional behaviour, while both resonance theory and FMO predictions fail to make this distinction (Figs. S8 and S15). Similarly, FMO theory fails to predict dominant reactivity in the 2-position of dibenzofuran **23** where the IE surface succeeds (Figs. 6a, S10 and S15).[52]

Borazarophenanthrenes have been shown to pose a particular challenge to many reactivity models, with FMO theory, the condensed Fukui function and atomic charge calculations all failing to predict the observed reactivity patterns (Fig. S15).[17, 18] IE surfaces are in agreement with the experimental data for compound **25**

(Fig. 6a and s14).[53-55] Similarly, IE surfaces give correct predictions of both the primary and secondary reactive sites in the recently prepared *N-tert*-butyl-*BN*-indole **25**.[56]

In some situations, IE minima may be highly localised mid-way between two atoms (Fig. 6b). Based on the observation that similar IE surfaces are displayed by alkenes, this suggests that molecules such as furan **26**, anthracene **27**, and phenanthrene **28** possess significant double-bond character. Consistent with this observation, these molecules are known to undergo oxidation and addition (Fig. 1c) as well as the usual substitution reactions (Fig. 6, and the references contained in Figs S8-S10 and S14). Interestingly, IE surfaces appear to allow olefinic and aromatic reactivity patterns to be separated. For example, while the IE minima lie over the 'double-bond' regions in molecules such as pyrene (Fig. S14) and anthracene **27**, the lowest average local IEs taken directly over the centre of each carbon atom at the molecular surface correspond to positions in which electrophilic aromatic substitution occurs (e.g. position 9 in anthracene **27**).

One further interesting curiosity is provided by compound **29**, whose central ring is best described as a cyclohexatriene with alternating single and double-bonds, rather than being benzenoid in character.[57, 58] In accord with the experimental observations, the IE minima lie over the double-bond regions in the central ring and not the outer aromatic rings (*cf.* terphenylene in Fig. S14). The IE surfaces calculated for the minimised and crystal structures of compound **29** are also sensitive to bond lengths and bending induced by crystal packing forces, giving local IE minima of 9.0 and 8.8 eV for each respective structure (Figs. 6 and S14).[59] Also of note is the similarity of the locations of IE minima in polycyclic aromatics compared to the recent direct observations of bond order obtained using noncontact atomic force microscopy.[60]

Conclusions

In summary, we have extracted reactivity patterns spanning over 150 years of synthetic developments in the field of aromatic chemistry and used the data to evaluate the predictive capacity of simple reactivity models. This large-scale systematic analysis has exposed numerous synthetically useful regioselectivities that are not predicted by many popular methods including resonance theory, FMO theory, the Fukui function, Brown's selectivity relationship, and electrostatic models. Many of these simple theoretical approaches fail to account for the reactivity of aromatic molecules because kinetic reactivity cannot usually be extrapolated from ground-state properties (such as HOMOs and ESPs, Fig. 2). Even though the Fukui function considers the changes in the HOMO coefficients between the ground-state and an intermediate resembling the transition-state formed in the rate-determining step, it still fails to account for the reactivity patterns observed in simple aromatic compounds.[18, 22, 23]

In contrast, we have shown that calculated average local ionisation energies (IEs) approximate the energy change accompanying the rate-determining step in the reactions of electrophiles with aromatic molecules

when steric demands are low (Fig. 3). Despite its simplicity, the IE method enables visualisation of the fundamental electronic factors governing reactivity in kinetically controlled aromatic reactions. Thus, we have highlighted numerous examples (Figs. 3-6) where reactivity predictions derived from resonance theory fail, but where IE surfaces succeed due to its apparent ability to take resonance, inductive effects and bond strain into account. Our analysis has therefore established IE surfaces as providing the most comprehensive simple rationalisation of aromatic reactivity to date. Since IE surfaces are both easily interpreted and provided as standard in popular computational chemistry software, we hope that the approach will assist in the development of new synthetic strategies, mechanistic understanding and chemical education.

References

[1] S. Couper, *Annales de Chimie et de Physique*, 1858, **53**, 469-489.

[2] A. Kekulé, *Bulletin de la Societe Chimique de Paris*, 1865, **3**, 98-110.

[3] G. W. Wheland, *J. Am. Chem. Soc.*, 1942, **64**, 900-908.

[4] L. P. Hammett, *J. Am. Chem. Soc.*, 1937, **59**, 96-103.

[5] L. Pauling and G. W. Wheland, *J. Chem. Phys.*, 1933, **1**, 362-374.

[6] K. Fukui, *Science*, 1982, **218**, 747-754.

[7] K. Fukui, T. Yonezawa and H. Shingu, *J. Chem. Phys.*, 1952, **20**, 722-725.

[8] R. J. Phipps and M. J. Gaunt, *Science*, 2009, **323**, 1593-1597.

[9] V. Snieckus, *Chem. Rev.*, 1990, **90**, 879-933.

[10] J. L. Gustafson, D. Lim and S. J. Miller, *Science*, 2010, **328**, 1251-1255.

[11] O. Allemann, S. Duttwyler, P. Romanato, K. K. Baldridge and J. S. Siegel, *Science*, 2011, **332**, 574-577.

[12] K. Godula and D. Sames, *Science*, 2006, **312**, 67-72.

[13] L. J. Goossen, G. Deng and L. M. Levy, *Science*, 2006, **313**, 662-664.

[14] J.-P. Corbet and G. Mignani, *Chem. Rev.*, 2006, **106**, 2651-2710.

[15] D.-H. Wang, K. M. Engle, B.-F. Shi and J.-Q. Yu, *Science*, 2010, **327**, 315-319.

[16] P. K. Weiner, R. Langridge, J. M. Blaney, R. Schaefer and P. A. Kollman, *Proc. Natl. Acad. Sci. USA*, 1982, **79**, 3754-3758.

[17] M. J. S. Dewar, *J. Mol. Struct.: THEOCHEM*, 1989, **59**, 301-323.

[18] J. S. M. Anderson, J. Melin and P. W. Ayers, *J. Chem. Theory Comput.*, 2007, **3**, 375-389.

[19] P. Perez, L. R. Domingo, M. Duque-Norena and E. Chamorro, *J. Mol. Struct.: THEOCHEM*, 2009, **895**, 86-91.

[20] M. Liljenberg, T. Brinck, B. Herschend, T. Rein, G. Rockwell and M. Svensson, *J. Org. Chem.*, 2010, **75**, 4696 - 4705.

[21] G. Koleva, B. Galabov, J. I. Wu, H. F. Schaefer, III and P. v. R. Schleyer, *J. Am. Chem. Soc.*, 2009, **131**, 14722-14727.

[22] W. Langenaeker, K. Demel and P. Geerlings, *J. Mol. Struct.: THEOCHEM*, 1991, **80**, 329-342.

[23] P. Fuentealba, E. Florez and W. Tiznado, *J. Chem. Theory Comput.*, 2010, **6**, 1470-1478.

[24] P. W. Atkins, T. L. Overton, J. P. Rourke and M. T. Weller, *Shriver & Atkins' Inorganic Chemistry*, Oxford University Press, Oxford, UK, 2010.

[25] P. Sjoberg, J. S. Murray, T. Brinck and P. Politzer, *Can. J. Chem.*, 1990, **68**, 1440-1443.

[26] C. Hansch, A. Leo and R. W. Taft, *Chem. Rev.*, 1991, **91**, 165-195.

[27] T. B. Phan, M. Breugst and H. Mayr, *Angew. Chem., Int. Ed.*, 2006, **45**, 3869-3874.

[28] R. G. Coombes, D. H. G. Crout, J. G. Hoggett, R. B. Moodie and K. Schofield, *J. Chem. Soc. B*, 1970, 347-357.

[29] D. R. Harvey and R. O. C. Norman, *J. Chem. Soc.*, 1961, 3604-3610.

[30] K. Tanemura, T. Suzuki, Y. Nishida, K. Satsumabayashi and T. Horaguchi, *Chem. Lett.*, 2003, **32**, 932-933.

[31] A. S. Lindsey and H. Jeskey, *Chem. Rev.*, 1957, **57**, 583-620.

[32] R. Neumann and Y. Sasson, *Synthesis*, 1986, **1986**, 569-570.

[33] J. F. Johnston, J. H. Ridd and J. P. B. Sandall, *Chem. Commun.*, 1989, 244-246.

[34] E. Baciocchi, F. Cacace, G. Ciranni and G. Illuminati, *J. Am. Chem. Soc.*, 1972, **94**, 7030-7034.

[35] S. Rozen, M. Brand and R. Lidor, *The Journal of Organic Chemistry*, 1988, **53**, 5545-5547.

[36] S. Rozen and D. Zamir, *J. Org. Chem.*, 1990, **55**, 3552-3555.

[37] G. S. Hammond and K. J. Douglas, *J. Am. Chem. Soc.*, 1959, **81**, 1184-1187.

[38] J. C. Smith, *J. Chem. Soc. B*, 1934, 213-218.

[39] P. L. Harris and J. C. Smith, *J. Chem. Soc.*, 1936, 168-168.

[40] I. Fleming, *Frontier Orbitals and Organic Chemical Reactions*, Wiley, London, 1978.

[41] H. Gilow and G. Walker, *J. Org. Chem.*, 1967, **32**, 2580-2583.

[42] P. Strazzolini, A. G. Giumanini, A. Runcio and M. Scuccato, *J. Org. Chem.*, 1998, **63**, 952-958.

[43] L. M. Stock, H. C. Brown and V. Gold, in *Adv. Phys. Org. Chem.*, Academic Press, 1963, vol. Volume 1, pp. 35-154.

[44] G. Koleva, B. Galabov, H. F. Schaefer, III and P. v. R. Schleyer, *J. Org. Chem.*, 2010, **75**, 2813-2819.

[45] S. M. Anatolii, *Rus. Chem. Rev.*, 1988, **57**, 144.

[46] X. Peng, N. Fukui, M. Mizuta and H. Suzuki, *Org. Biomol. Chem.*, 2003, **1**, 2326-2335.

[47] C. Barnett, *Chem. Commun.*, 1967, 637.

[48] P. Bélanger, *Tetrahedron Lett.*, 1979, **20**, 2505-2508.

[49] S. Schroeter and T. Bach, *Heterocycles*, 2007, **74**, 569-594.

[50] S. Schroeter and T. Bach, *Synlett*, 2005, 1957-1959.

[51] H. Oda, T. Hanami, T. Iwashita, M. Kojima, M. Itoh and Y. Hayashizaki, *Tetrahedron*, 2007, **63**, 12747-12753.

[52] T. Keumi, N. Tomioka, K. Hamanaka, H. Kakihara, T. Morita, H. Kitajima and M. Fukushima, *J. Org. Chem.*, 1991, **56**, 4671-4677.

[53] M. J. S. Dewar and V. P. Kubba, *J. Am. Chem. Soc.*, 1961, **83**, 1757-1760.

[54] M. J. S. Dewar and V. P. Kubba, *Tetrahedron*, 1959, **7**, 213-222.

[55] M. J. S. Dewar and V. P. Kubba, *J. Org. Chem.*, 1960, **25**, 1722-1724.

[56] E. R. Abbey, L. N. Zakharov and S.-Y. Liu, *J. Am. Chem. Soc.*, 2010, **132**, 16340–16342.

[57] H.-D. Beckhaus, R. Faust, A. J. Matzger, D. L. Mohler, D. W. Rogers, C. Rüchardt, A. K. Sawhney, S. P. Verevkin, K. P. C. Vollhardt and S. Wolff, *J. Am. Chem. Soc.*, 2000, **122**, 7819-7820.

[58] D. L. Mohler, K. P. C. Vollhardt and S. Wolff, *Angew Chem. Int. Ed. Eng.*, 1995, **34**, 563-565.

[59] D. Holmes, S. Kumaraswamy, A. J. Matzger and K. P. C. Vollhardt, *Chem. Eur. J.*, 1999, **5**, 3399-3412.

[60] L. Gross, F. Mohn, N. Moll, B. Schuler, A. Criado, E. Guitián, D. Peña, A. Gourdon and G. Meyer, *Science*, 2012, **337**, 1326-1329.